LWT - Food Science and Technology 184 (2023) 115024

Contents lists available at ScienceDirect

LWT

journal homepage: www.elsevier.com/locate/lwt

Interaction of iron(III) with taste enhancers: Potential of Fe(III) salts with inosine monophosphate or guanosine monophosphate for food fortification

Judith Bijlsma [a], Péter Buglyó [b], Etelka Farkas [b], Krassimir P. Velikov [c,d,e], Jean-Paul Vincken [a], Wouter J.C. de Bruijn [a,*]

[a] Laboratory of Food Chemistry, Wageningen University & Research, Bornse Weilanden 9, P.O. Box 17, 6700 AA, Wageningen, the Netherlands
[b] Department of Inorganic and Analytical Chemistry, University of Debrecen, H-4032, Debrecen, Egyetem tér 1, Hungary
[c] Unilever Innovation Centre Wageningen B.V, Bronland 14, 6708 WH, Wageningen, the Netherlands
[d] Institute of Physics, University of Amsterdam, Science Park 904, 1098 XH, Amsterdam, the Netherlands
[e] Soft Condensed Matter, Debye Institute for Nanomaterials Science, Utrecht University, Princetonplein 5, 3584 CC, Utrecht, the Netherlands

ARTICLE INFO

Keywords:
Ferric
Polyphenol
Metal chelation
Nucleotides
Flavor enhancers

ABSTRACT

Iron interactions in iron-fortified savory concentrates lead to undesirable discoloration, even when poorly-water soluble iron salts such as ferric pyrophosphate (Fe_4PP_3) are used. This is the first study to comprehensively investigate the interaction of Fe(III) with three common taste enhancers: glutamate (Glu), inosine monophosphate (IMP), and guanosine monophosphate (GMP). The stability of the complexes of Fe(III) with IMP or GMP is higher compared to that with Glu. Neutrality of IMP or GMP species with Fe(III) at pH 3–8 resulted in precipitation. This property was exploited to synthesize Fe(III) salts of IMP or GMP (i.e. Fe_2IMP_3 and Fe_2GMP_3) by aqueous chemical precipitation. Iron dissolution from Fe_2IMP_3 and Fe_2GMP_3 was up to twenty-fold higher at gastric pH (1–3), indicative of better bio-accessibility, and up to fifteen-fold lower at food pH (3–7), indicative of decreased reactivity in food, compared to Fe_4PP_3. Consequently, Fe_2IMP_3 and Fe_2GMP_3, compared to Fe_4PP_3, led to less discoloration in combination with the poorly soluble phenolics that are commonly present in savory concentrates. We conclude that Fe(III) salts of IMP or GMP can potentially serve as iron fortificants due to their increased solubility at gastric pH (1–3), decreased iron dissolution at food pH (3–7), and decreased reactivity at food pH.

1. Introduction

Fortification of savory concentrates (e.g. bouillon cubes) with iron can effectively reduce the global prevalence of iron deficiency (de Mejia, Aguilera-Gutiérrez, Martin-Cabrejas, & Mejia, 2015; Hurrell, 1997; Moretti et al., 2006). Bouillon cubes are typically composed of salt, fat, carbohydrates, proteins, herbs, and spices. Additionally, they may contain taste enhancers. The most widely used taste enhancer in food is the monosodium salt of glutamate (MSG, NaGlu; E621), which is often used in combination with the disodium salts of 5′-ribonucleotides such as guanosine 5′-monophosphate (Na_2GMP; E626) and inosine 5′-monophosphate (Na_2IMP; E630), to further boost the umami taste (Acebal, Lista, & Fernández Band, 2008; Chiang, Yen, & Mau, 2007). For example, dry bouillon cubes from different local supermarkets in Argentina contained 38 ± 17% (w/w) MSG, 0.23 ± 0.16% (w/w) IMP, and 0.06 ± 0.05% (w/w) of GMP (Acebal et al., 2008).

When a savory concentrate is fortified with iron, the product color and iron bioavailability can be compromised due to iron-phenolic interactions (Bijlsma, de Bruijn, Velikov, & Vincken, 2022; Gupta et al., 2020; Habeych, van Kogelenberg, Sagalowicz, Michel, & Galaffu, 2016). These phenolics are naturally present in the herbs (Bijlsma, de Bruijn, et al., 2023; Hostetler, Riedl, & Schwartz, 2012). To counter these reactions, insoluble iron fortificants, such as ferric pyrophosphate (i.e. ferric diphosphate; Fe_4PP_3), are used for the fortification of bouillon

Abbreviations: EDX, energy dispersive X-ray spectroscopy; GMP, guanosine monophosphate; HILIC-PDA-ESI-ITMS^n, hydrophilic interaction liquid chromatography coupled to electrospray ionization ion trap mass spectrometry; Glu, glutamate; ICP-AES, inductively coupled plasma atomic emission spectroscopy; IMP, inosine monophosphate; MSG, monosodium glutamate; MP, monophosphate; PP, pyrophosphate; SEM, scanning electron microscopy; TEM, transmission electron microscopy; UV–Vis, ultraviolet–visible; XRD, X-ray diffraction.

* Corresponding author.
E-mail address: wouter.debruijn@wur.nl (W.J.C. de Bruijn).

https://doi.org/10.1016/j.lwt.2023.115024
Received 24 March 2023; Received in revised form 6 June 2023; Accepted 24 June 2023
Available online 3 July 2023

cubes (Gupta et al., 2020; Martínez-Navarrete, Camacho, Martínez-Lahuerta, Martí;nez-Monzó, & Fito, 2002). Fe_4PP_3 is practically insoluble (<0.1 mg/L) in aqueous solution at pH 3–5 and sparingly soluble (10–33 mg/L) at pH 1–2 (Allen, De Benoist, Dary, & Hurrell, 2006; Moslehi et al., 2022; Tian, Blanco, Smoukov, Velev, & Velikov, 2016). Despite its water insolubility at food pH discoloration with phenolics can still be observed in the presence of Fe_4PP_3 (Allen et al., 2006; Bijlsma, Moslehi, et al., 2023; Dueik, Chen, & Diosady, 2017; Hurrell et al., 2004).

The presence of glutamate (Glu) was previously associated with increased discoloration in an iron-phenolic model system and an iron-fortified savory food concentrate (Bijlsma et al., 2020; Jansen & Velikov, 2014). Ferric iron (Fe(III)) was previously reported to coordinate to glutamate via the carboxylate oxygen atoms (Djurdjević & Jelić, 1997). Additionally, nucleotides strongly coordinate metals, although the metal binding preference is metal and nucleobase dependent (Lopez & Liu, 2017; Thakur et al., 2018; Zhou, Shi, Yao, Sheng, & Li, 2015). Metal ions may be coordinated to nucleotides via the oxygen donor atoms of the phosphate group, the nitrogen atom in the nucleobase, the oxygen atoms of the sugar moiety, or a combination thereof (Alabart, Moreno, Labarta, Tejada, & Molins, 1990; Aoki, 1976; Aoki, Clark, & Orbell, 1976). As hard Lewis metals prefer to coordinate to hard Lewis ligands such as the phosphate group, it is expected that Fe(III) primarily coordinates to the phosphate groups of the nucleotides (Moreno et al., 1985; Richter & Fischer, 2003; Zhelyaskov & Yue, 1992). The pH plays a crucial role in the coordination of metals to ligands because it affects the ligand protonation state and hydrolysis of the metals. Nevertheless, the effect of pH on the coordination of Fe(III) to IMP or GMP and the resulting speciation in aqueous systems was not reported to date. Knowledge of the type of coordination complexes (e.g. stability, coordination mode, solubility) formed by Fe(III) with taste enhancers at different pH values will help to understand the reactivity of Fe(III) in (fortified) savory foods.

Here we comprehensively study the interaction of Fe(III) and all taste enhancers in aqueous solution at different pH. IMP and GMP are expected to coordinate Fe(III) via their phosphate group, therefore, we also included monophosphate (MP) and pyrophosphate (PP) for comparison. Fe_4PP_3 is one of the most commonly used salts in iron fortification but, despite its wide use, data regarding the basic properties, formed complexes, stability constants, and solubility are inconsistent (Atkári, Kiss, Bertani, & Martin, 1996; Jiang, Wang, Parekh, & Leonard, 1998; Lemire, Taylor, Schlenz, & Palmer, 2020; Rossi, Velikov, & Philipse, 2014; Sun, Zhao, & Teng, 2020; Tian et al., 2016). In general Fe(III) phosphates form neutral insoluble complexes in aqueous solution in the food pH range (3–7) (Allen et al., 2006; Moslehi et al., 2022; Tian et al., 2016). Since IMP and GMP also coordinate Fe(III) via the phosphate group, we expect that their complexes with iron will also be insoluble in aqueous solution at food pH (3–7).

This work aims to provide more insight into the interaction of Fe(III) with Glu, IMP, GMP, MP, and PP in aqueous solutions as influenced by pH. The effect of pH on coordination, speciation, and solubility of the complexes in aqueous model systems was elucidated by pH-potentiometric and UV–Vis spectrophotometric methods. These techniques are widely used because they allow determination of the stability constants and stoichiometry of metal-ligand complexes at different pH values (Malacaria et al., 2021). We hypothesized that (i) all taste enhancers coordinate Fe(III) but that, due to the hard Lewis nature of the phosphate groups, IMP, GMP, MP, and PP form more stable complexes with Fe(III) compared to Glu, and (ii) that complexes of Fe(III) with IMP, GMP, MP, and PP possess limited solubility at food pH (3–7) due to coordination via the phosphate group.

2. Materials and methods

2.1. Materials

Ferric chloride hexahydrate ($FeCl_3{\cdot}6H_2O$; a.r. grade) was purchased from Reanal (Budapest, Hungary). The following ligands were purchased from Merck Life Science (Darmstadt, Germany): pyrophosphate (PP) tetrasodium salt decahydrate (Na_4PP, $Na_4P_2O_7{\cdot}10H_2O$, purity ≥99%), dihydrogen phosphate (MP) monosodium salt monohydrate (NaH_2MP, $NaH_2PO_4{\cdot}H_2O$, purity ≥99%), L-glutamate (Glu) monosodium salt monohydrate (NaHGlu, $NaC_5H_8NO_4{\cdot}H_2O$, purity ≥98%), inosine 5′-monophosphate (IMP) disodium salt hydrate (Na_2IMP, $Na_2C_{10}H_{11}N_4O_8P{\cdot}xH_2O$, purity ≥99%), and guanosine 5′-monophosphate (GMP) disodium salt hydrate (Na_2GMP, $Na_2C_{10}H_{12}N_5O_8P{\cdot}xH_2O$, purity ≥99%). Ferric chloride ($FeCl_3$, purity ≥97%, for synthesis), quercetin hydrate (purity ≥95%), 1,2-dihydroxybenzene (purity ≥99%; catechol), caffeic acid (purity ≥98%), curcumin (purity ≥94%), 3-(2-pyridyl)-5,6-diphenyl-1,2,4-triazine-*p*,*p*′-disulfonic acid monosodium salt hydrate (purity ≥97%; ferrozine), hydrochloric acid (HCl), and potassium hydroxide (KOH) were also purchased from Merck Life Science. (−)-Epicatechin (purity ≥97%) was purchased from TCI Europe NV (Zwijndrecht, Belgium), apigenin (purity ≥98%) from Indofine Chemical Company (Hillsborough, NJ, USA), and ascorbic acid (purity ≥99%) was obtained from VWR International (Radnor, PA, USA). ULC-MS grade acetonitrile (ACN) and water both containing 0.1% (v/v) formic acid, and pure formic acid (FA, purity ≥99%) were purchased from Biosolve (Valkenswaard, The Netherlands). Water for other purposes than UHPLC was prepared using a Milli-Q water purification system (Merck Millipore, Billerica, MA, USA).

2.2. Potentiometric and spectrophotometric studies

2.2.1. Preparation of the solutions

The metal ion stock solutions for pH-potentiometric and spectrophotometric measurements were prepared from $FeCl_3{\cdot}6H_2O$ (Reanal, Hungary), the stock solution also contained 0.10 mol/L hydrochloric acid to prevent hydrolysis. Metal ion concentrations were determined by complexometric titration. The acid content of Fe(III) stock solution and the purity and exact concentration of the ligand stock solutions were determined by Gran's method (Gran, Dahlenborg, Laurell, & Rottenberg, 1950).

Due to the limited water solubility of some of the Fe(III) complexes, pH-potentiometric and spectrophotometric measurements were carried out in aqueous solution (water) and also in DMSO/water 70/30% (w/w).

2.2.2. Potentiometric measurements

All pH-potentiometric measurements were carried out at an ionic strength of 0.20 mol/L (KCl) and at 25.0 ± 0.1 °C. A carbonate-free KOH solution of known concentration (0.20 mol/L) in water or the solvent mixture was used as titrant. HCl stock solutions in water or the solvent mixture were prepared and their concentrations were determined by potentiometric titrations.

A Mettler T50 instrument equipped with a Metrohm combined electrode (type 6.0234.100) and Metrohm T5 instrument with Metrohm combined electrode (type DG1114-SC) were used for the pH-potentiometric measurements. The IUPAC recommendations were employed to perform the measurements in the DMSO/water 70/30% (w/w) solvent mixture. The combined glass electrode was conditioned in the solvent mixture for three days before the measurements (Mussini, Covington, Longhi, & Rondinini, 1985). The electrode system was

calibrated according to Irving et al., pH-metric readings could therefore be converted into hydrogen ion concentration (Irving, Miles, & Pettit, 1967). The water ionization constant (pK_w) was 13.74 ± 0.01 in the aqueous system and 17.01 ± 0.01 in the solvent mixture. The titrations in aqueous solution were performed in the pH range of 2.0–11.0 and in solvent mixture in the pH range of 3.0–15.0 or until precipitation occurred. The initial volume of the samples was 15.0 mL. Ligand concentrations were kept constant at 4.0 mmol/L and the Fe(III) to ligand ratios were 1:1, 1:2, 1:4 and 1:10. All samples were completely deoxygenated by bubbling with purified argon for ca. 15 min before the measurements.

2.2.3. Interpretation of potentiometric data

The protonation constants of the ligands were determined with the computer program SUPERQUAD (Sabatini, Vacca, & Gans, 1974). Potentiometric data were used to determine the stoichiometry of the species and calculate their stability constants. These calculations were performed using the computer program PSEQUAD (Gans, Sabatini, & Vacca, 1996) and the literature data (log β) for hydrolytic Fe(III) species, taking into account the different ionic strengths by the Davies equation. The following values were used in the calculations: $[FeH_{-1}]^{2+} = -3.21$; $[FeH_{-2}]^{+} = -6.73$; $[Fe_2H_{-2}]^{4+} = -4.09$; and $[Fe_3H_{-4}]^{5+} = -7.58$; H_{-1} relates to the metal induced ionization of the coordinated water (Baes & Mesmer, 1977; Farkas, Buglyó, Enyedy, Gerlei, & Santos, 2002). Titration points with a waiting time of 10 min or more were omitted from the calculations and about 200 titration points were used for each system.

2.2.4. Spectrophotometric measurements

UV-spectra of the Fe(III) containing systems in aqueous solution were recorded using a PerkinElmer Lambda 25 spectrophotometer. Iron (III) ion concentrations were in the range of 0.025–0.10 mmol/L and the metal ion to ligand ratios were in the range of 1:3–1:6. Measurements were carried out in the range of 0.7–11.0 or until precipitation occurred. Measurements were carried out by preparing individual samples in which the 0.20 mol/L KCl was partially or completely replaced by HCl. The pH values, varying in the range of ca. 0.7–1.6, were calculated from the HCl content. UV–Vis spectra were recorded over the range of 200–800 nm with a path length of 1 cm.

2.3. Preparation of Fe_4PP_3, Fe_2IMP_3, and Fe_2GMP_3 salts

Iron(III)-IMP ($Fe_2(C_{10}H_{11}N_4O_8P)_3$; Fe_2IMP_3) and iron(III)-GMP ($Fe_2(C_{10}H_{12}N_5O_8P)_3$; Fe_2GMP_3) salts were separately prepared using an aqueous chemical precipitation method as described elsewhere (Moslehi et al., 2022). Iron(III)-pyrophosphate ($Fe_4(P_2O_7)_3$; Fe_4PP_3) was also prepared for comparison.

The net precipitation reactions of the three different salts are indicated by **equations (1)–(3)**.

$$Fe_4PP_3 : 4FeCl_{3\,(aq)} + 3Na_4P_2O_{7(aq)} \rightarrow Fe_4(P_2O_7)_{3(s)} + 12NaCl_{(aq)} \quad \text{Eq.1}$$

$$Fe_2IMP_3 : 2FeCl_{3(aq)} + 3Na_2IMP_{(aq)} \rightarrow Fe_2IMP_{3(s)} + 6NaCl_{(aq)} \quad \text{Eq.2}$$

$$Fe_2GMP_3 : 2FeCl_{3(aq)} + 3Na_2GMP_{(aq)} \rightarrow Fe_2GMP_{3(s)} + 6NaCl_{(aq)} \quad \text{Eq.3}$$

The reactions were performed at room temperature by mixing the following stoichiometric ratios of the reactants: 4:3.1 for Fe_4PP_3 and 2:3.1 for Fe_2IMP_3 and Fe_2GMP_3. A small excess of the ligand solution was added to ensure binding of all iron, i.e. 3.1 times instead of 3 in **eqs. (1)–(3)**. For Fe_2IMP_3 and Fe_2GMP_3, solutions of 2.07 mmol $FeCl_3$ in 250 mL MQ water were prepared. Subsequently, they were quickly added to solutions of 3.22 mmol Na_2IMP or Na_2GMP in 500 mL of MQ water while stirring at 500 r/min. For Fe_4PP_3, a solution of 4.15 mmol $FeCl_3$ in 250 mL MQ water was quickly added to a solution of $Na_4(P_2O_7)$ (3.22 mmol, 500 mL) while stirring at 500 r/min. For all three systems, a turbid dispersion was rapidly formed upon mixing. Freshly prepared solutions were used for every synthesis and two independent syntheses were performed for each salt. The dispersions were then centrifuged (6000×*g*, 25 °C, 45 min) in 500 mL centrifuge bottles followed by washing the precipitates twice with Milli-Q water to remove the aqueous NaCl. The sediments were dried in a vacuum oven at 50 °C overnight (Fe_2IMP_3: 27 ± 2% yield; Fe_2GMP_3: 50 ± 0% yield; Fe_4PP_3: 46 ± 10% yield). The salts were characterized by XRD, TEM, SEM-EDX, and by elemental analysis (CHNS, ICP-AES) (supplementary information, **method SI-1**).

2.4. Iron dissolution and reactivity of Fe_4PP_3, Fe_2IMP_3, and Fe_2GMP_3 salts

2.4.1. Iron dissolution from Fe_4PP_3, Fe_2IMP_3, and Fe_2GMP_3

The Fe_4PP_3, Fe_2IMP_3, and Fe_2GMP_3 salts were redispersed in Milli-Q water to obtain final concentrations of 10 mg/mL. The pH of the dispersions was adjusted by automatic titration with 0.1 mol/L HCl or 0.1 mol/L NaOH in a pH-stat device (Metrohm, Herisau, Switzerland). The dispersions were incubated at 1000 r/min using an Eppendorf Thermomixer® F1.5 (Eppendorf, Hamburg, Germany) at pH values ranging from one to eleven (steps of one), for 2 h at 23 °C. After incubation, the pH of each sample was measured again to determine the final pH. The samples were centrifuged at 15,000×*g* for 10 min and supernatants were isolated to measure the dissolved iron concentrations. Total iron in solution was quantified using a ferrozine-based colorimetric assay as reported previously (Moslehi et al., 2022). All measurements were performed in duplicate and quantification of total dissolved iron was performed based on intensity ($A_{565\ nm}$) with a calibration curve of $FeSO_4$ (0.0078–1 mmol/L, $R^2 > 0.99$).

2.4.2. Reactivity of Fe_4PP_3, Fe_2IMP_3, and Fe_2GMP_3 with phenolics

The reactivity of Fe_4PP_3, Fe_2IMP_3, and Fe_2GMP_3 salts with phenolics was assessed according to our previously published method with slight modifications (Bijlsma, Moslehi, et al., 2023). To this end, three water soluble phenolics (i.e. catechol, caffeic acid, and epicatechin) and three poorly water soluble phenolics (i.e. quercetin, apigenin, and curcumin) were investigated. The reactivity of Fe_4PP_3, Fe_2IMP_3, and Fe_2GMP_3 in the presence of the different phenolic compounds after incubation at pH 6.5 for 2 h at 23 °C, was monitored using ultraviolet–visible light (UV–Vis) spectroscopy and the dissolved iron resulting from phenolic interactions was quantified using a ferrozine-based colorimetric assay (Moslehi et al., 2022).

2.5. Nucleotide and nucleoside quantification by HILIC-PDA-ESI-ITMS^n

To investigate if dephosphorylation occurred we analyzed the nucleotides and nucleosides by hydrophilic interaction liquid chromatography coupled to electrospray ionization ion trap mass spectrometry (HILIC-PDA-ESI-ITMS^n). The injection volume, column information, temperature, gradient elution program, and MS settings were used as described in the supplementary information (**Method SI-2**).

2.6. Statistical analyses

Selection of the equilibrium models in SUPERQUAD and PSEQUAD (section 2.2.3) was based on critical analysis of the weighted residuals, the statistical parameters (χ^2, σ), and graphical comparisons between the experimental and simulated potentiometric curves (Gans et al., 1996; Sabatini et al., 1974). For the potentiometric titrations at least three ratios of metal:ligand were tested and the standard deviations of the potentiometric data after processing with SUPERQUAD and PSEQUAD are indicated as 3σ values (i.e. data within three standard deviations from the mean, thus covering 99.7% of the data), the standard deviations over the last decimal are indicated in parentheses; *i.e,* 9.49(1) equals 9.49 ± 0.01.

The Fe_2IMP_3 and Fe_2GMP_3 and Fe_4PP_3 salts were prepared as independent duplicates. The resulting images from characterization by XRD,

TEM, and SEM are displayed for one of the duplicates after a reproducibility check. The dissolution, reactivity, elemental composition, and dephosphorylation were measured in duplicate and are indicated as average ± standard deviation of the duplicate measurements. To assess whether the change in phenolic recovery was statistically significant, ANOVA was performed using IBM SPSS Statistic v23 software (SPSS Inc., Chicago, IL, USA). Tukey's *post hoc* comparisons (significant at $p < 0.05$) were performed to evaluate the difference in the soluble iron concentration compared to the other iron salts with the same phenolic.

3. Results and discussion

3.1. Interaction of iron(III) with taste enhancers and phosphates

3.1.1. Proton equilibria of the ligands

The fully protonated ligands H_3MP and $H_3(Glu)^+$ have three dissociable protons and H_4PP, $H_3(IMP)^+$, and $H_3(GMP)^+$ have four dissociable protons (Fig. 1).

The corresponding dissociation constants of the ligands in aqueous solutions were determined by pH-potentiometric titrations at the same conditions (25 °C, 0.20 mol/L KCl) as used to investigate the interaction with Fe(III) (Table 1).

Since the pH-effect of the deprotonation processes is not sensitive for the dissociation sites, if a compound has more than one dissociable proton, the dissociation constants (so called macro-constants) determined by pH-potentiometric method cannot be assigned to the individual sites; assumptions can only be made based on chemical evidence. For the compounds in this study, the acidity orders are known from literature and described in more detail in the paragraph below.

It was previously described that for $H_3(IMP)^+$ and $H_3(GMP)^+$ the first proton is released from the phosphate, the second from *N*7 on the nucleobase, the third from the phosphate, and the fourth from *N*1 (at alkaline pH) (Gogia, Jain, & Puranik, 2009; Sigel, Massoud, & Corfu, 1994). For H_3Glu^+ it was previously reported that the first proton is released from the α-carboxylate, the second from the γ-carboxylate, and the third from the α-amino group (Bastug et al., 2011). Taking the different experimental conditions into account, the dissociation constants of the ligands are in reasonable agreement with the reported data in literature (Atkári et al., 1996; Djurdjević et al., 1997; Kiss et al., 1995; Sigel et al., 1994).

The hydrolytic stability of IMP, GMP, and PP was monitored by a second titration similar to what was done previously (Éva A. Enyedy, Pócsi, & Farkas, 2004; Oivanen & Lonnberg, 1990). After the titration of IMP, GMP, and PP with KOH titrant up to pH around 12, HCl was added to set the pH at 2 again after which the sample was titrated with KOH again. The obtained titration curves were superimposed (results not shown) and therefore indicate that IMP, GMP, and PP do not hydrolyze in aqueous solution in the measured pH range during the run time of one titration (i.e. several hours).

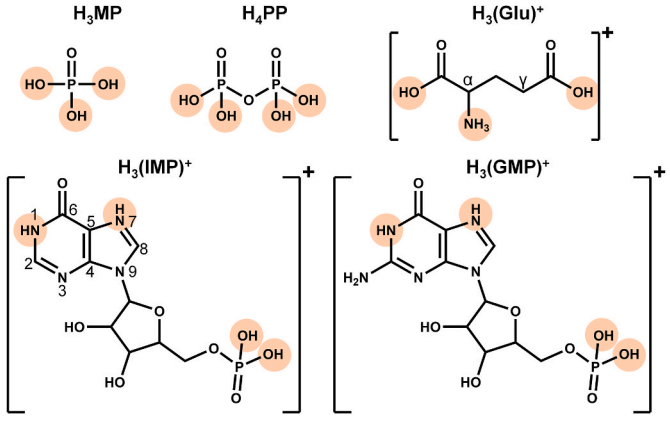

Fig. 1. Chemical structure of monophosphate (MP), pyrophosphate (PP), glutamate (Glu), inosine 5′-monophosphate (IMP), and guanosine 5′-monophosphate (GMP) in their protonated state. The orange circles highlight the dissociable protons. (For interpretation of the references to color in this figure legend, the reader is referred to the Web version of this article.)

Table 1
Dissociation constants of the studied ligands determined by pH-potentiometric titrations (T = 25.0 °C, I = 0.20 mol/L (KCl) in aqueous solution).

	$H_3(Glu)^+$	$H_3(IMP)^+$	$H_3(GMP)^+$	H_3MP	H_4PP
pK_1	2.11(2)[a]	<1[b]	<1	1.78(1)	<1
pK_2	4.08(1)	1.19(2)	2.18(3)	6.64(1)	1.54(1)
pK_3	9.49(1)	6.09(1)	6.08(2)	11.57(1)	5.84(1)
pK_4		8.94(1)	9.39(1)		8.19(1)

[a] Standard deviations (3σ values) of the last decimal are given in parentheses.
[b] It was not possible to measure at pH < 1 using the potentiometric setup but it is known that the first pK_a of these compounds is at very acidic pH (Atkári et al., 1996; Djurdjević et al., 1997; Kiss et al., 1995; Sigel et al., 1994).

3.1.2. Investigation of Fe(III) complexes of the ligands by potentiometric titration

The pH-potentiometric titrations of Fe(III) with all ligands were performed in aqueous solution (water) and in the solvent mixture (DMSO/water 70/30% (w/w)) and were terminated when precipitation occurred. For the system of Fe(III) in presence of MP at a 1:4 ratio precipitation occurred at pH > 3.5 (supplementary information, Fig. SI-1). The Fe(III) systems with PP displayed white precipitate from the start (i.e. pH 2) for all measured ratios (i.e. 1:1, 1:2, and 1:4). Due to the low dissociation constants (Table 1) and bidentate binding, PP already forms stable chelates with Fe(III) at acidic pH.

The pH-potentiometric titration curves of the taste enhancers Glu, IMP, and GMP with Fe(III) are provided in Fig. 2. The investigation of the Fe(III) complexes with all the taste enhancers was hindered by the very low solubility of the iron complexes and/or by the formation of iron hydrolysis products.

For the Fe(III) systems with Glu, orange-red precipitate was observed for all ratios. We suggest this is due to the formation of iron hydrolysis products which were previously reported to have this color (Flynn, 1984). When more ligand was present (1:4 ratio), precipitation occurred at a higher pH. These outcomes indicate that Glu competes with hydroxide for iron coordination. This was further confirmed by the 1:10 ratio sample, in which iron precipitated at an even higher pH. For IMP or GMP the titrations were terminated upon the formation of a white precipitate, we suggest that precipitation is a result of the coordination of Fe(III) to the phosphate anion in the nucleotides. For Fe(III) in presence of GMP the precipitate at 1:4 ratio was formed at pH > 3.0 and for IMP at pH > 4.7. It is interesting that for GMP the precipitation occurs at lower pH compared to IMP because the only structural difference between these ligands is the presence of $–NH_2$ for GMP, and this amine is unlikely to coordinate Fe(III) (Lopez et al., 2017).

The experimental potentiometric data of the Fe(III) complexes within the pH range in which no precipitation was observed was fitted using the PSEQUAD program. Due to the precipitation reactions, no acceptable fitting was obtained for complexes of Fe(III) with PP, IMP, and GMP. Thus, it was not possible to obtain quantitative data about the stoichiometries and stabilities of the complexes in these systems. For the complexes of Fe(III) with Glu and MP, acceptable fitting was obtained and the stability constants of these complexes are given in Table 2.

The model and the stability constants of the 1:1 species with different protonation degree obtained in the Fe(III)-Glu system were similar to those previously reported (Djurdjević et al., 1997). Calculations with MP indicated the formation of a 1:1 $FePO_4$ species. Including the previously reported 1:1 complexes $FeH_2PO_4^{2+}$ and $FeHPO_4^{+}$ (Lemire et al., 2020) into the model resulted in lower fitting parameters. It should be noted that stoichiometries of the species in Table 2 may cover mixed

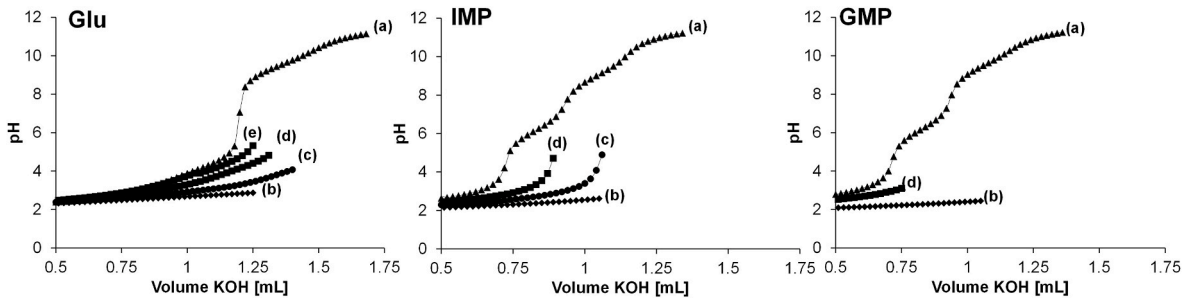

Fig. 2. pH-potentiometric titration curves in aqueous solution for 4.0 mmol/L Glu, IMP, and GMP in (**a**) absence and in presence of Fe(III) at a ratio of Fe(III):ligand (**b**) 1:1, (**c**) 1:2, (**d**) 1:4, and (**e**) 1:10 at I = 0.20 mol/L (KCl), and T = 25.0 °C.

Table 2
Protonation constants of Glu and MP and stability constants (Log β) of the Fe(III) complexes of Glu and MP determined by pH-potentiometric titrations (T = 25.0 °C, I = 0.20 mol/L (KCl) in aqueous solution).

Log β	Glu [a]	MP [a]
H_3L	15.68(2)	19.99(1)
H_2L	13.57(1)	18.21(1)
HL	9.49(1)	11.57(1)
[FeHL]	12.90(2)	–
[FeL]	10.82(6)	19.92(9)
[FeH_1L]	7.92(3)	–
Fitting[b]	0.0362	0.0305

[a] Standard deviations (3σ values) are in parentheses.
[b] Average difference between experimental and calculated titration curves expressed in cm^3 of titrant.

hydroxido complexes (e.g. FeL = [Fe(HL)(OH)]) in which, besides the differently protonated ligand, hydroxide ion(s) can also be found in the coordination sphere of the metal ion due to the high tendency of Fe(III) to hydrolyze.

Previously, stoichiometric data and stability constants of poorly water soluble ligands could be measured in DMSO/water mixtures (Éva A Enyedy et al., 2020; Éva A Enyedy et al., 2011). So, we also investigated if stability data of combinations of Fe(III) with the ligands could be obtained in a mixture of DMSO/water 70/30% (w/w). The dissociation constants of Glu, IMP, and MP in DMSO/water 70/30% (w/w) are given in supplementary information (**Tables SI–1**). Although the 1:1 combinations of Fe(III) with Glu, IMP, and GMP indicated slightly improved solubility in the solvent mixture, precipitation still occurred at pH 5.2, 3.9, and 3.4, respectively. Thus, the titration curves could not be acceptably fitted in PSEQUAD. These results implied that investigation of the systems of Fe(III) in presence of PP, IMP, or GMP by pH-potentiometric titrations was not possible due to the poor solubility of these ligands and their ready complexation at very acidic pH. Poor solubility is the main limitation for quantitative evaluation of the complexes of these ligands with Fe(III), as it hinders pH-potentiometric titration. Therefore, the speciation was further investigated by spectrophotometric analysis.

3.1.3. Investigation of Fe(III) complexes of the ligands by spectrophotometry

Qualitative information about the speciation was obtained by spectrophotometry (Fig. 3). With spectrophotometric measurements the acidic pH region in aqueous solution can be extended to a pH around 0.7 and measurements can be carried out at a lower concentration of metal and ligand, thus precipitation is less likely.

At pH 0.7–1.5 monochloro complexes of Fe(III) (i.e. $[FeCl]^{2+}$) were identified by the typical absorption band with a λ_{max} of 334–336 nm

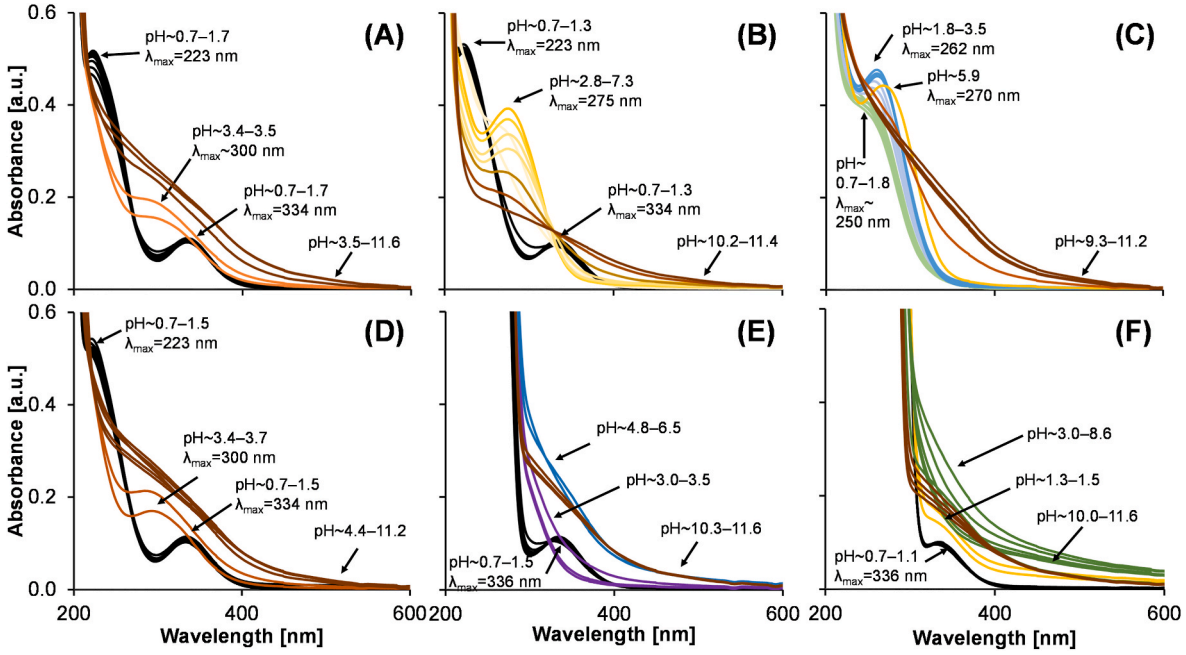

Fig. 3. Representative UV–Vis absorption spectra of the Fe(III) system in (**a**) absence of ligand and in presence of (**b**) MP, (**c**) PP, (**d**) Glu, (**e**) IMP, and (**f**) GMP at different pH values ($C_{Fe(III)}$ = 0.1 mmol/L, C_{Ligand} = 0.4 mmol/L, and I = 0.20 mol/L (KCl)).

both for $FeCl_3$ without ligands and in the systems in presence of MP, Glu, IMP, or GMP (Bjerrum & Lukes, 1986; Heistand & Clearfield, 1963). $FeCl_3$ solution without ligand or in presence of MP and Glu also showed the typical $[FeCl]^{2+}$ band at 223 nm, which was not observed in presence of IMP or GMP, most likely due to overlap with the intense absorbance of the nucleotides at < 280 nm.

In absence of ligand or in presence of Glu, a band with λ_{max} ~300 nm was observed at pH 3.4–3.5, corresponding to the hydrolytic products $[Fe(OH)]^{2+}$ or $[Fe_2(OH)_2]^{4+}$ (Gá Lente & Fábián, 2001). At pH > 3.5, in absence of ligand and in the presence of Glu, a broad band from 200 to 600 nm was observed. This band is a result of the formation of the red-orange colored (hydr)oxide species (Flynn, 1984). Formation of this band for Fe(III) (hydr)oxide species was hindered by the presence of the ligands with a phosphate group (MP, PP, IMP, and GMP) until pH > 10. However, it cannot be ruled out that other (colorless) mixed (hydr)oxide species are present.

In the presence of MP a band with a λ_{max} at 275 nm was observed from pH 2.8 to 7.3, this corresponds to the 1:1 species of Fe(III) with MP (i.e. $[FeH_2PO_4]^{2+}$)(Gábor Lente, Magalhães, & Fábián, 2000). In presence of PP a band with a shoulder at 250 nm was present at pH 0.7, which indicates that at pH 0.7 the complexation of Fe(III) by PP is already complete. In presence of PP a band with a λ_{max} at 262 nm was formed at pH 1.8–3.5 and at pH ~5.9 a band with λ_{max} at 270 nm was present. We suggest that these bands correspond to the formation of $[FeH_3P_2O_7]^{2+}$, $[FeH_2P_2O_7]^{+}$, and $Fe_4(P_2O_7)_3$, respectively (Jiang et al., 1998).

The fact that similar spectra were obtained in presence of Glu as for $FeCl_3$ in absence of ligand, indicates that there were only weak interactions of Glu with Fe(III) at these concentrations. Previously, at higher concentrations of Fe(III) and Glu, a change in absorbance was reported at a λ_{max} of 450 nm (Djurdjević et al., 1997). We confirmed that in a more highly concentrated Fe(III) and Glu system (i.e. 30 mmol/L Glu and 3 mmol/L Fe(III)) a species with a poorly defined maximum around 450 nm at pH ~ 3 was formed (supplementary information, Fig. SI-2). Formation of this species indicates that at higher Glu and Fe (III) concentrations there is a competition between the carboxylate moieties of glutamic acid and hydroxide for iron coordination. The interaction of Fe(III) with carboxylate is weaker than that of Fe(III) with hydroxide due to the lower electron density of the conjugated base pair of the carboxylate compared to the hydroxide. If present in high concentrations, as in some savory concentrates (e.g. 38% (w/w) MSG) (Acebal et al., 2008), the carboxylate moieties of Glu may be able to compete with hydroxide and coordinate Fe(III) at low pH.

In presence of IMP or GMP, the formation of a soluble species at pH ~3 was followed by the formation of a second poorly soluble species as indicated by the increase of the baseline around 700–800 nm. Based on the dissociation constants of IMP and GMP (Table 1) we suggest that the soluble species of IMP or GMP at pH ~ 3 could be due to the formation of a soluble macrochelate of Fe(III) with GMP or IMP via coordination to the deprotonated phosphate and *N7*, as previously reported for these ligands in the presence of divalent metals (Sigel et al., 1994). Alternatively, these species may be stabilized by secondary interactions such as hydrogen bonding or stacking when *N7* is deprotonated. The insoluble species that are formed at pH > 4.8 for IMP and pH > 3 for GMP are more likely to result from the formation of charge neutral coordination complexes of Fe(III) with the phosphate group. These spectrophotometric results are in line with the potentiometric titrations in which precipitation of Fe(III) with GMP was also observed at lower pH compared to Fe(III) with IMP.

The stability of the complexes of Fe(III) with IMP or GMP is higher compared to Glu, as they form species at lower ratios of ligand (1:1), whereas for Glu higher concentrations ligand (1:10) are needed to compete with the hydroxide for coordination. Moreover, our results indicate that the presence of IMP or GMP can hinder the formation of the red-orange colored Fe(III) (hydr)oxide species up to pH > 10. The fact that IMP or GMP can form water soluble Fe(III) species at pH < 3 (i.e. gastric pH) but insoluble Fe(III) species at pH 3–7 (i.e. food pH) makes them promising iron salts for fortification of foods (Allen et al., 2006; Moslehi et al., 2022; Tian et al., 2016). Therefore, we decided to synthesize and characterize salts of Fe(III) and IMP or GMP.

3.2. Synthesis and characterization of Fe_4PP_3, Fe_2IMP_3, and Fe_2GMP_3 salts

To investigate the potential of insoluble salts of Fe(III) with IMP, GMP, and PP as iron fortificants with a decreased reactivity we synthesized Fe_4PP_3, Fe_2IMP_3, and Fe_2GMP_3 salts using an aqueous chemical precipitation method. The Fe_4PP_3, Fe_2IMP_3, and Fe_2GMP_3 salts were characterized by XRD, TEM, SEM-EDX, ICP-AES, and the elemental analyzer (see **supplementary information** for a detailed description of the results per analysis). The dried Fe(III) salts had different colors (Fig. 4a); Fe_4PP_3 was white, Fe_2IMP_3 was yellow, and Fe_2GMP_3 orange. XRD analyses of the Fe_4PP_3, Fe_2IMP_3, and Fe_2GMP_3 salts indicated that they were all amorphous (Fig. 4b).

With TEM analysis, these amorphous particles were confirmed, although different types of shapes and particle sizes were observed (Fig. 4c, Fig. SI-3). Fe_4PP_3 consisted of aggregates of colloidal particles typical for precipitation with sizes from 5 to 30 nm, which is in line with previous reports (Rossi et al., 2014; van Leeuwen, Velikov, & Kegel, 2012). Fe_2IMP_3 consisted of aggregates of spherical particles with an average size of 100 nm, whereas Fe_2GMP_3 aggregates consisted of more elongated primary particles with an average size of 50 nm. We suggest that differently shaped particles were created for GMP because it can form G-quadruplexes that are cross-linked by Fe(III) to assemble into larger coordination polymers (supplementary information, Fig. SI-4) (Bhattacharyya, Saha, & Dash, 2018; Sutyak, Zavalij, Robinson, & Davis, 2016; Thakur et al., 2019; Xiao & Davis, 2018). Homogenous distribution of the elements in the salts was confirmed by SEM-EDX (Fig. SI-6). A high abundance of H as detected in the elemental analysis (**Tables SI–2**) indicated that the salts were hydrated. Furthermore, the analyzed elemental ratios were in good agreement with the calculated elemental ratios (**Tables SI–3**) based on the molecular formulas for stoichiometric ratios as provided in **Method 2.3**.

3.3. pH-dependent dissolution behavior and iron-phenolic reactivity

3.3.1. pH-dependent iron dissolution from Fe_4PP_3, Fe_2IMP_3, and Fe_2GMP_3

For food fortification purposes it is important that iron salts possess pH-dependent dissolution behavior. To limit iron-mediated reactions, while maximizing bio-accessibility, iron dissolution from the iron salts should be limited in the pH range of food (3–7) and fast at gastric (1–3) and/or intestinal pH (6–8). Therefore the pH-dependent dissolution behavior of iron from Fe_4PP_3, Fe_2IMP_3, and Fe_2GMP_3 salts was investigated (Fig. 5). It can be observed that Fe_4PP_3 possessed low solubility in the acidic pH range (1–4), whereas the iron dissolution increases around pH 4. For Fe_2IMP_3, iron dissolution from the salt was observed at pH < 3 and pH > 6. Similarly, Fe_2GMP_3 also possessed iron dissolution at pH < 3 and at pH > 6.5.

Up to a fifteen-fold decrease of soluble iron for Fe_2IMP_3 and Fe_2GMP_3 at food pH (3–7) was observed compared to Fe_4PP_3. This dissolution behavior makes Fe_2IMP_3 and Fe_2GMP_3 desirable as fortification salts for food, as it could potentially lead to reduced iron-mediated reactivity in the food products since less iron is in solution. Moreover, the up to a twenty-fold increase in iron solubility of Fe_2IMP_3 and Fe_2GMP_3 salts in the gastric pH range (1–3), compared to Fe_4PP_3, are indicative of better bio-accessibility in the gastric environment (Hurrell, 2002; Moslehi et al., 2022; Rohner et al., 2007; Tian et al., 2016). At intestinal pH (6–8) the Fe_2IMP_3 and Fe_2GMP_3 salts show a decrease in solubility compared to Fe_4PP_3. However, the solubility in acid is the common measure used to indicate bio-accessibility (Allen et al., 2006), and was shown to be a good indication for *in vivo* iron uptake (Rohner et al., 2007).

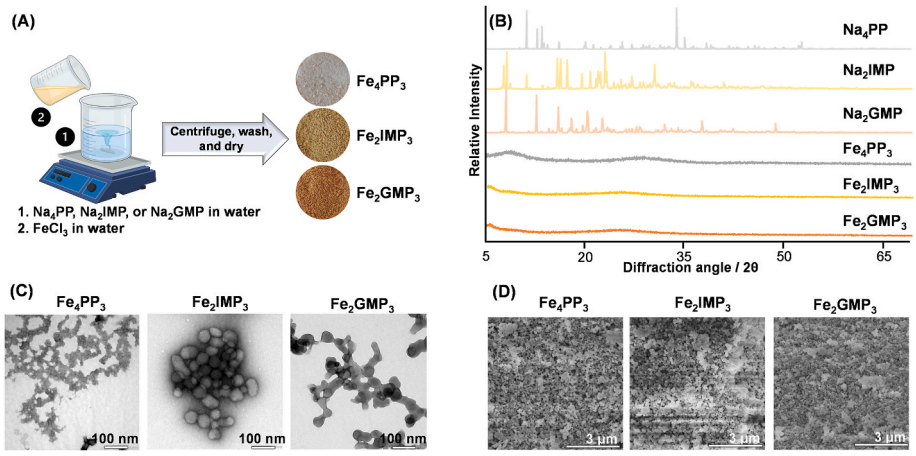

Fig. 4. (**a**) Synthesis of iron-containing salts via an aqueous chemical precipitation procedure and color of the dried salts; (**b**) Powder XRD patterns of the ligands before and after reacting with iron; (**c**) TEM and (**d**) SEM images of Fe_4PP_3, Fe_2IMP_3, and Fe_2GMP_3. (For interpretation of the references to color in this figure legend, the reader is referred to the Web version of this article.)

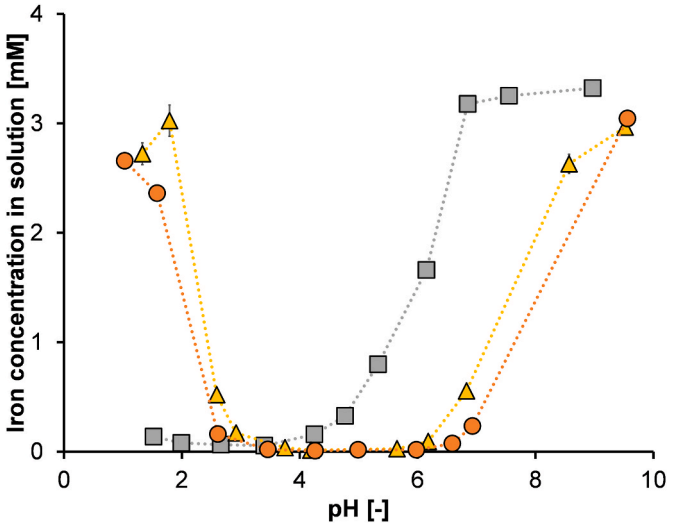

Fig. 5. Iron dissolution from Fe_4PP_3 (grey square), Fe_2IMP_3 (yellow triangle), and Fe_2GMP_3 (orange circle) as a function of pH. Error bars indicate the standard deviation of independent duplicates. (For interpretation of the references to color in this figure legend, the reader is referred to the Web version of this article.)

3.3.2. *Reactivity of Fe_4PP_3, Fe_2IMP_3, and Fe_2GMP_3 with phenolics*

Besides the iron dissolution from the iron salts, we also evaluated the reactivity of the iron salts with phenolics. Prevention of iron-phenolic interactions is important to ensure iron bio-accessibility and limit discoloration (McGee & Diosady, 2018). For these phenolic reactivity measurements, we applied a set of six model phenolic compounds with different chemical properties, most notably different water solubilities, as previously reported (Bijlsma, Moslehi, et al., 2023). Fig. 6 shows the total absorbance, color, and iron in a solution of the three salts after incubation with different phenolics at pH 6.5 (2 h, 23 °C). This pH was chosen as it is in the pH range of savory concentrates. For the water soluble phenolics (i.e. catechol, caffeic acid, and epicatechin) an absorbance band at λ_{max} ~580 nm was observed for all three salts. This absorbance at 580 nm is indicative for 1:2 complexes of Fe(III) from the salts with the catecholate moiety of the phenolic, and is responsible for the bluish to purplish appearance (Fig. 6b) (Bijlsma et al., 2020; Elhabiri, Carrër, Marmolle, & Traboulsi, 2007). It was observed that in presence of the water soluble phenolics the total absorbance and discoloration in the Fe_2IMP_3 and Fe_2GMP_3 samples was equal or even showed a slight increase compared to Fe_4PP_3. This was contrary to our expectations, because much lower iron solubilities for Fe_2IMP_3 and Fe_2GMP_3 salts in aqueous solution were observed at pH 6.5 in Fig. 5. However, we also measured the iron solubilities of the salts in presence of the phenolics and noticed a fast increase in iron dissolution from the salt in presence of the water soluble phenolics compared to the insoluble phenolics (Fig. 6c). As suggested previously, the water soluble phenolics may coordinate Fe(III) on the surface of the insoluble salt particles and thereby bring it in solution, forming soluble colored complexes (Bijlsma, Moslehi, et al., 2023). This interaction of Fe(III) with phenolics can compete with the Fe(III) interactions with PP, IMP, and GMP at neutral pH because the phenolate oxygens are more electron-rich compared to the phosphate oxygens. In general, very strong coordinate bonds with Fe (III) are formed for highly electron-rich binding sites (Athira, Mann, Sharma, Pothuraju, & Bajaj, 2021).

In presence of quercetin and curcumin, absorbance in the visible spectra increased and discoloration of the samples was observed in presence of Fe_4PP_3 (Fig. 6a and **b**). For Fe_2IMP_3 and Fe_2GMP_3 with these phenolics, no increased absorbances of the supernatants were observed. The precipitate changed from a yellow to brownish color. We hypothesized previously that the discoloration of these precipitates can be due to formation of Fe(III)-phenolic complexes on the surface of the salts (Bijlsma, Moslehi, et al., 2023). For apigenin, no absorbance was observed with any of the Fe(III) salts. These poorly water soluble phenolics do not increase the Fe(III) dissolution (Fig. 6c) from the surface of the salts and therefore no discoloration was observed for Fe_2IMP_3 and Fe_2GMP_3 in aqueous solutions at pH 6.5. These findings indicate that Fe_2IMP_3 and Fe_2GMP_3 are promising salts for the fortification of food products containing poorly soluble phenolic compounds, such as the phenolics that are commonly present in bouillon cubes.

3.4. *Dephosphorylation of GMP and IMP in presence of Fe(III)*

Dephosphorylation of nucleoside 5′-mono, -di-, and -triphosphates was previously reported to be catalyzed by metal coordination (Buisson & Sigel, 1974; Oivanen et al., 1990; Sigel, 1990). To check if dephosphorylation occurred in the Fe(III) salts of the nucleotides, we separated and quantified the amounts of nucleotides and nucleosides in the synthesized salts of Fe_2IMP_3 and Fe_2GMP_3 using HILIC-PDA-MS^n (supplementary information, Fig. SI-7). We observed a small peak for inosine and guanosine but for both salts >98% of the total peak area was still the intact nucleotide. This indicates that the nucleotides are stable in a coordination complex with Fe(III).

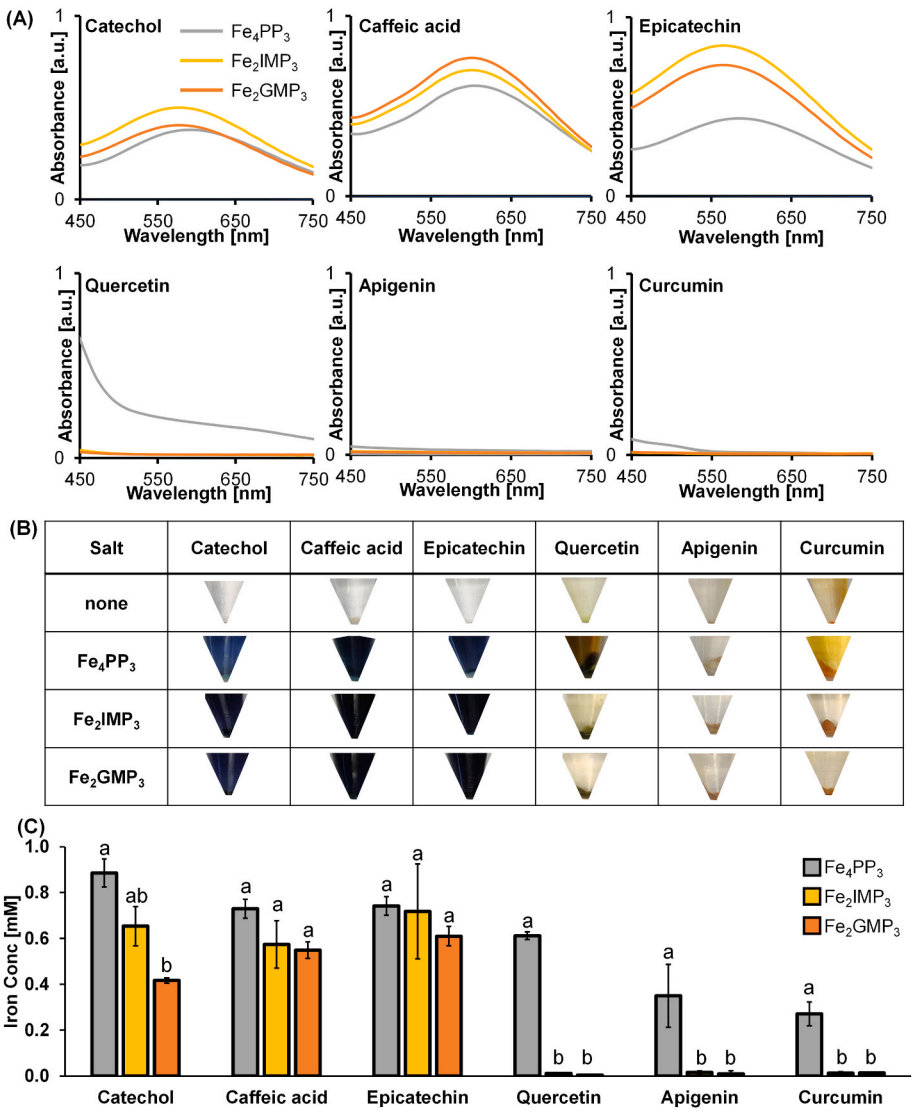

Fig. 6. (**a**) Absorbance spectra of the supernatants of Fe_4PP_3, Fe_2IMP_3, and Fe_2GMP_3 in the presence of different phenolics at pH 6.5. (**b**) Pictures of the samples in the Eppendorf tubes after incubation and centrifugation. (**c**) Soluble iron concentration in solutions of Fe_4PP_3, Fe_2IMP_3, and Fe_2GMP_3 after incubation (2 h, pH 6.5) with different phenolics. Error bars indicate the standard deviation of independent duplicates. Different letters indicate a significant difference in the soluble iron concentration compared to the other iron salts with the same phenolic (Tukey's test, $p < 0.05$).

3.5. Implications of iron fortification using Fe_2IMP_3 and Fe_2GMP_3

The main findings of our work are that the Fe(III) salts of IMP or GMP can potentially serve as food fortificants because of their pH-dependent iron dissolution, i.e. increased iron dissolution at gastric pH (1–3) and decreased iron dissolution at food pH (3–7). This results in decreased reactivity with poorly soluble phenolics that are commonly present in savory concentrates, whilst maintaining bio-accessibility. However, for successful fortification of foods with these salts, their effect on sensorial properties and iron bioavailability are also important parameters.

The effect of Fe(III) coordination to IMP and GMP on the sensorial properties of these taste enhancers, specifically their umami perception has to be confirmed in future sensory studies. We expect that the coordination of Fe(III) to IMP or GMP may affect their interaction with the umami receptor because the negatively charged phosphate group is normally involved in stabilization of that interaction (Zhang et al., 2008).

Previously, we have also synthesized mixed Ca–Fe(III) pyrophosphate salts that already possessed very promising dissolution behavior (Moslehi et al., 2022). Compared to the Ca–Fe(III) pyrophosphate salts, these nucleotide salts are even five times more soluble in the gastric pH range and two times less soluble in the food pH range. Additionally, the presence of dietary nucleotides has already been demonstrated to enhance the intestinal absorption of iron in rats (Cosgrove, 1998; Faelli & Esposito, 1970). However, additional experiments have to be performed to confirm the bioavailability of iron from the Fe_2IMP_3 and Fe_2GMP_3 salts. Based on the increased dissolution of Fe_2IMP_3 and Fe_2GMP_3 at gastric pH, our work implies that these salts may be preferred over Fe_4PP_3 and Ca–Fe(III) pyrophosphate salts as iron fortificants.

4. Conclusions

This is the first study that reports the pH-dependent interaction of taste enhancers (Glu, IMP, and GMP) and phosphates (MP and PP) with Fe(III) in aqueous solutions. All three taste enhancers can coordinate Fe (III), however, coordination was more stable with the phosphate moiety of the nucleotides (IMP and GMP) than with the carboxylate moieties of glutamate (Glu). Similar to complexes of Fe(III) with PP, complexes of Fe (III) with IMP or IMP possess limited solubility in aqueous solution at pH 3–8, leading to their precipitation. The precipitation of these species with Fe(III) was utilized to synthesize salts of Fe(III) with IMP, GMP, and PP using an aqueous chemical precipitation method. The synthesized Fe (III) salts of IMP or GMP possessed increased iron dissolution at gastric pH (1–3), decreased iron dissolution at food pH (3–7), and less discoloration with poorly soluble phenolics compared to the currently used fortification salt Fe_4PP_3. In conclusion, these Fe(III) salts with IMP or GMP have the potential to be used to design more stable iron-fortified foods.

Funding sources

This work was performed in the public–private partnership "IRON-TECH" and was financed by participating industrial partners Unilever Innovation Centre Wageningen B.V., Nouryon Chemicals B.V., Nobian B. V., and allowances of The Netherlands Organization for Scientific Research (NWO) in the framework of the Innovation Fund for Chemistry and from the Ministry of Economic Affairs in the framework of the "*TKI/PPS-Toeslagregeling*" (Grant 731017205).

CRediT authorship contribution statement

Judith Bijlsma: Conceptualization, Methodology, Investigation, Visualization, Writing – original draft. **Péter Buglyó:** Supervision, Methodology, Writing – review & editing. **Etelka Farkas:** Writing – review & editing. **Krassimir P. Velikov:** Conceptualization, Supervision, Writing – review & editing. **Jean-Paul Vincken:** Conceptualization, Supervision, Writing – review & editing. **Wouter J.C. de Bruijn:** Conceptualization, Supervision, Writing – review & editing.

Declaration of competing interest

The authors declare the following financial interests/personal relationships which may be considered as potential competing interests. Judith Bijlsma, Wouter J.C. de Bruijn, Krassimir P. Velikov, and Jean-Paul Vincken are inventors on a patent filed on a food product comprising multivalent metal ion salts of nucleotides and wish to mention that this compound may have further potential as commercial fortificant for food.

Data availability

Data will be made available on request.

Acknowledgements

We would like to thank Orsolya Bogdányi-Fekete for her support with the potentiometric measurements, and the Department of Inorganic and Analytical Chemistry at the University of Debrecen for hosting Judith Bijlsma. We are thankful to the Graduate School VLAG for granting the PhD fellowship to visit Debrecen University. We thank Neshat Moslehi (Utrecht University) for the fruitful discussion on the synthesis of the Fe(III) salts. We would like to thank Jelmer Vroom from the Wageningen Electron Microscopy Centre (WEMC) for carrying out TEM and SEM data collection and Ilse Gerrits (Wageningen University & Research) for her help with the X-Ray powder diffraction measurements. The authors are grateful to Arjen Reichwein, Johan Hoekstra, and Ewout Otto of Nouryon Specialty Chemicals B.V. for performing the elemental analysis. Part of the presented results were obtained using advanced microscopy, mass spectrometry, and XRD equipment which is owned by WUR-Shared Research Facilities. Investment by WUR-Shared Research Facility was made possible by the 'Regio Deal Foodvalley' of the province of Gelderland, The Netherlands.

Appendix A. Supplementary data

Supplementary data to this article can be found online at https://doi.org/10.1016/j.lwt.2023.115024.

References

Acebal, C. C., Lista, A. G., & Fernández Band, B. S. (2008). Simultaneous determination of flavor enhancers in stock cube samples by using spectrophotometric data and multivariate calibration. *Food Chemistry, 106*, 811–815. https://doi.org/10.1016/j.foodchem.2007.06.009

Alabart, J. R., Moreno, V., Labarta, A., Tejada, J., & Molins, E. (1990). Electronic structure determination and dynamical properties of iron (II)-guanosine-5′-monophosphate complex via mossbauer and magnetic susceptibility measurements. *The Journal of Chemical Physics, 92*, 6131–6139. https://doi.org/10.1063/1.458336

Allen, L. H., De Benoist, B., Dary, O., & Hurrell, R. (2006). *Guidelines on food fortification with micronutrients*. World Health Organization.

Aoki, K. (1976). Crystallographic studies of interactions between nucleotides and metal ions. II. The crystal and molecular structure of the 1: 1 complex of cadmium (II) with guanosine 5'-phosphate. *Acta Crystallographica Section B Structural Crystallography and Crystal Chemistry, 32*, 1454–1459. https://doi.org/10.1107/S0567740876005554

Aoki, K., Clark, G. R., & Orbell, J. D. (1976). Metal-phosphate bonding in transition metal·nucleotide complexes. The crystal and molecular structures of the polymeric copper(II) complex of guanosine 5′-monophosphate. *Biochimica et Biophysica Acta (BBA) - Nucleic Acids and Protein Synthesis, 425*, 369–371. https://doi.org/10.1016/0005-2787(76)90264-1

Athira, S., Mann, B., Sharma, R., Pothuraju, R., & Bajaj, R. K. (2021). Preparation and characterization of iron-chelating peptides from whey protein: An alternative approach for chemical iron fortification. *Food Research International, 141*. https://doi.org/10.1016/j.foodres.2021.110133. article 110133.

Atkári, K., Kiss, T., Bertani, R., & Martin, R. B. (1996). Interactions of aluminum(III) with phosphates. *Inorganic Chemistry, 35*, 7089–7094. https://doi.org/10.1021/ic960329e

Baes, C. F., & Mesmer, R. S. (1977). The hydrolysis of cations. *Berichte der Bunsen-Gesellschaft für Physikalische Chemie, 81*, 245–246. https://doi.org/10.1002/bbpc.19770810252

Bastug, A. S., Goz, S. E., Talman, Y., Gokturk, S., Asil, E., & Caliskan, E. (2011). Formation constants and coordination thermodynamics for binary complexes of Cu (II) and some α-amino acids in aqueous solution. *Journal of Coordination Chemistry, 64*, 281–292. https://doi.org/10.1080/00958972.2010.541454

Bhattacharyya, T., Saha, P., & Dash, J. (2018). Guanosine-derived supramolecular hydrogels: Recent developments and future opportunities. *ACS Omega, 3*, 2230–2241. https://doi.org/10.1021/acsomega.7b02039

Bijlsma, J., de Bruijn, W. J. C., Hageman, J. A., Goos, P., Velikov, K. P., & Vincken, J.-P. (2020). Revealing the main factors and two-way interactions contributing to food discolouration caused by iron-catechol complexation. *Scientific Reports, 10*. https://doi.org/10.1038/s41598-020-65171-1. article 8288.

Bijlsma, J., de Bruijn, W. J. C., Koppelaar, J., Sanders, M. G., Velikov, K. P., & Vincken, J.-P. (2023). *Interactions of natural flavones with iron are affected by 7-O-glycosylation, but not by additional 6″-O-acylation*. ACS Food Science & Technology. https://doi.org/10.1021/acsfoodscitech.3c00112

Bijlsma, J., de Bruijn, W. J. C., Velikov, K. P., & Vincken, J.-P. (2022). Unravelling discolouration caused by iron-flavonoid interactions: Complexation, oxidation, and formation of networks. *Food Chemistry, 370*. https://doi.org/10.1016/j.foodchem.2021.131292. article 131292.

Bijlsma, J., Moslehi, N., Velikov, K. P., Kegel, W. K., Vincken, J.-P., & de Bruijn, W. J. C. (2023). Reactivity of Fe(III)-containing pyrophosphate salts with phenolics: Complexation, oxidation, and surface interaction. *Food Chemistry, 407*. https://doi.org/10.1016/j.foodchem.2022.135156. article 135156.

Bjerrum, J., & Lukes, I. (1986). The iron (III)-chloride system. A study of the stability constants and of the distribution of the tetrachloro species between organic solvents and aqueous chloride solutions. *Acta Chemica Scandinavica, 40a*, 31–40. https://doi.org/10.3891/acta.chem.scand.40a-0031

Buisson, D. H., & Sigel, H. (1974). Significance of binary and ternary copper(II) complexes for the promotion and protection of adenosine 5′-di- and triphosphate toward hydrolysis. *Biochimica et Biophysica Acta (BBA) - General Subjects, 343*, 45–63. https://doi.org/10.1016/0304-4165(74)90238-4

Chiang, P.-D., Yen, C.-T., & Mau, J.-L. (2007). Non-volatile taste components of various broth cubes. *Food Chemistry, 101*, 932–937. https://doi.org/10.1016/j.foodchem.2006.02.041

Cosgrove, M. (1998). *Nucleotides. Nutrition, 14*, 748–751. https://doi.org/10.1016/S0899-9007(98)00075-6

Djurdjević, P., & Jelić, R. (1997). Solution equilibria in L-glutamic acid and L-serine+ iron(III) systems. *Transition Metal Chemistry, 22*, 284–293. https://doi.org/10.1023/A:1018476810838

Dueik, V., Chen, B. K., & Diosady, L. L. (2017). Iron-polyphenol interaction reduces iron bioavailability in fortified tea: Competing complexation to ensure iron bioavailability. *Journal of Food Quality*. https://doi.org/10.1155/2017/1805047, 2017, article 1805047.

Elhabiri, M., Carrër, C., Marmolle, F., & Traboulsi, H. (2007). Complexation of iron(III) by catecholate-type polyphenols. *Inorganica Chimica Acta, 360*, 353–359. https://doi.org/10.1016/j.ica.2006.07.110

Enyedy, É. A., May, N. V., Pape, V. F., Heffeter, P., Szakács, G., Keppler, B. K., et al. (2020). Complex formation and cytotoxicity of triapine derivatives: A comparative solution study on the effect of the chalcogen atom and NH-methylation. *Dalton Transactions, 49*, 16887–16902. https://doi.org/10.1039/D0DT03465G

Enyedy, É. A., Pócsi, I., & Farkas, E. (2004). Complexation of desferricoprogen with trivalent Fe, Al, Ga, in and divalent Fe, Ni, Cu, Zn metal ions: Effects of the linking chain structure on the metal binding ability of hydroxamate based siderophores. *Journal of Inorganic Biochemistry, 98*, 1957–1966. https://doi.org/10.1016/j.jinorgbio.2004.08.017

Enyedy, É. A., Primik, M. F., Kowol, C. R., Arion, V. B., Kiss, T., & Keppler, B. K. (2011). Interaction of triapine and related thiosemicarbazones with iron (III)/(II) and gallium (III): A comparative solution equilibrium study. *Dalton Transactions, 40*, 5895–5905. https://doi.org/10.1039/C0DT01835J

Faelli, A., & Esposito, G. (1970). Effect of inosine and its metabolites on intestinal iron absorption in the rat. *Biochemical Pharmacology, 19*, 2551–2554. https://doi.org/10.1016/0006-2952(70)90003-1

Farkas, E., Buglyó, P., Enyedy, É. A., Gerlei, V. A., & Santos, A. M. (2002). Factors affecting the metal ion–hydroxamate interactions: Effect of the position of the peptide function in the connecting chain on the Fe(III), Mo(VI) and V(V) complexation of some new desferrioxamine B (DFB) model dihydroxamic acids. *Inorganica Chimica Acta, 339*, 215–223. https://doi.org/10.1016/S0020-1693(02)00932-5

Flynn, C. M. (1984). Hydrolysis of inorganic iron(III) salts. *Chemical Reviews, 84*, 31–41, 0.1021/cr00059a003.

Gans, P., Sabatini, A., & Vacca, A. (1996). Investigation of equilibria in solution. Determination of equilibrium constants with the HYPERQUAD suite of programs. *Talanta, 43*, 1739–1753. https://doi.org/10.1016/0039-9140(96)01958-3

Gogia, S., Jain, A., & Puranik, M. (2009). Structures, ionization equilibria, and tautomerism of 6-oxopurines in solution. *The Journal of Physical Chemistry B, 113*, 15101–15118. https://doi.org/10.1021/jp9057753

Gran, G., Dahlenborg, H., Laurell, S., & Rottenberg, M. (1950). Determination of the equivalent point in potentiometric titrations. *Acta Chemica Scandinavica, 4*, 559–577. https://doi.org/10.1039/AN9527700661

Gupta, S., Habeych, E., Scheers, N., Merinat, S., Rey, B., Galaffu, N., et al. (2020). The development of a novel ferric phytate compound for iron fortification of bouillons (part I). *Scientific Reports, 10*. https://doi.org/10.1038/s41598-020-61833-2. article 5340.

Habeych, E., van Kogelenberg, V., Sagalowicz, L., Michel, M., & Galaffu, N. (2016). Strategies to limit colour changes when fortifying food products with iron. *Food Research International, 88*, 122–128. https://doi.org/10.1016/j.foodres.2016.05.017

Heistand, R. N., & Clearfield, A. (1963). The effect of specific swamping electrolytes upon the formation constant of the monochloroiron (III) complex. *Journal of the American Chemical Society, 85*, 2566–2570. https://doi.org/10.1021/ja00900a007

Hostetler, G. L., Riedl, K. M., & Schwartz, S. J. (2012). Endogenous enzymes, heat, and pH affect flavone profiles in parsley (*Petroselinum crispum* var. *neapolitanum*) and celery (*Apium graveolens*) during juice processing. *Journal of Agricultural and Food Chemistry, 60*, 202–208. https://doi.org/10.1021/jf2033736

Hurrell, R. F. (1997). Preventing iron deficiency through food fortification. *Nutrition Reviews, 55*, 210–222. https://doi.org/10.1111/j.1753-4887.1997.tb01608.x

Hurrell, R. F. (2002). How to ensure adequate iron absorption from iron-fortified food. *Nutrition Reviews, 60*, S7–S15. https://doi.org/10.1301/002966402320285137

Hurrell, R. F., Lynch, S., Bothwell, T., Cori, H., Glahn, R., Hertrampf, E., et al. (2004). Enhancing the absorption of fortification iron. *International Journal for Vitamin and Nutrition Research, 74*, 387–401. https://doi.org/10.1024/0300-9831.74.6.387

Irving, H., Miles, M., & Pettit, L. (1967). A study of some problems in determining the stoicheiometric proton dissociation constants of complexes by potentiometric titrations using a glass electrode. *Analytica Chimica Acta, 38*, 475–488. https://doi.org/10.1016/S0003-2670(01)80616-4

Jansen, F. J. H. M., & Velikov, K. P. (2014). *Fortified savoury food concentrate, EP2774497B1*. European Patent Office.

Jiang, C., Wang, X., Parekh, B., & Leonard, J. (1998). Pyrite depression by phosphates in coal flotation. *Mining, Metallurgy & Exploration, 15*, 1–7. https://doi.org/10.1007/BF03402779

Kiss, T., Buglyó, P., Sanna, D., Micera, G., Decock, P., & Dewaele, D. (1995). Oxovanadium(IV) complexes of citric and tartaric acids in aqueous solution. *Inorganica Chimica Acta, 239*, 145–153. https://doi.org/10.1016/0020-1693(95)04750-6

van Leeuwen, Y. M., Velikov, K. P., & Kegel, W. K. (2012). Morphology of colloidal metal pyrophosphate salts. *RSC Advances, 2*, 2534–2540. https://doi.org/10.1039/C2RA00449F

Lemire, R., Taylor, P., Schlenz, H., & Palmer, D. (2020). *Chemical thermodynamics of iron, part 2. Boulogne-Billancourt*. France: Nuclear Energy Agency of the OECD (NEA).

Lente, G., & Fábián, I. (2001). A simple test to confirm the ligand substitution reactions of the hydrolytic iron(III) dimer. *Reaction Kinetics and Catalysis Letters, 73*, 117–125. https://doi.org/10.1023/A:1013941308447

Lente, G., Magalhães, M. E. A., & Fábián, I. (2000). Kinetics and mechanism of complex formation reactions in the iron(III)−phosphate ion system at large iron(III) excess. Formation of a tetranuclear complex. *Inorganic Chemistry, 39*, 1950–1954. https://doi.org/10.1021/ic991017p

Lopez, A., & Liu, J. (2017). Self-assembly of nucleobase, nucleoside and nucleotide coordination polymers: From synthesis to applications. *ChemNanoMat, 3*, 670–684. https://doi.org/10.1002/cnma.201700154

Malacaria, L., Corrente, G. A., Beneduci, A., Furia, E., Marino, T., & Mazzone, G. (2021). A review on coordination properties of Al(III) and Fe(III) toward natural antioxidant molecules: Experimental and theoretical insights. *Molecules, 26*, 2603. https://doi.org/10.3390/molecules26092603

Martínez-Navarrete, N., Camacho, M. M., Martínez-Lahuerta, J., Martínez-Monzó, J., & Fito, P. (2002). Iron deficiency and iron fortified foods—a review. *Food Research International, 35*, 225–231. https://doi.org/10.1016/S0963-9969(01)00189-2

McGee, E. J. T., & Diosady, L. L. (2018). Prevention of iron-polyphenol complex formation by chelation in black tea. *LWT - Food Science and Technology, 89*, 756–762. https://doi.org/10.1016/j.lwt.2017.11.041

de Mejia, E. G., Aguilera-Gutiérrez, Y., Martin-Cabrejas, M. A., & Mejia, L. A. (2015). Industrial processing of condiments and seasonings and its implications for micronutrient fortification. *Annals of the New York Academy of Sciences, 1357*, 8–28. https://doi.org/10.1111/nyas.12869

Moreno, V., Terrón, A., Vicens, M., Molins, E., Labarta, A., Caubet, A., et al. (1985). Synthesis, spectroscopic and magnetic characterization of some iron(III)-nucleotide compounds. *Transition Metal Chemistry, 10*, 90–93. https://doi.org/10.1007/BF00618455

Moretti, D., Zimmermann, M. B., Wegmüller, R., Walczyk, T., Zeder, C., & Hurrell, R. F. (2006). Iron status and food matrix strongly affect the relative bioavailability of ferric pyrophosphate in humans. *The American Journal of Clinical Nutrition, 83*, 632–638. https://doi.org/10.1093/ajcn.83.3.632

Moslehi, N., Bijlsma, J., De Bruijn, W. J. C., Velikov, K. P., Vincken, J.-P., & Kegel, W. K. (2022). Design and characterization of Ca-Fe(III) pyrophosphate salts with tunable pH-dependent solubility for dual-fortification of foods. *Journal of Functional Foods, 92*. https://doi.org/10.1016/j.jff.2022.105066. article 105066.

Mussini, T., Covington, A., Longhi, P., & Rondinini, S. (1985). Criteria for standardization of pH measurements in organic solvents and water + organic solvent mixtures of moderate to high permittivities. *Pure and Applied Chemistry, 57*, 865–876. https://doi.org/10.1351/pac198557060865

Oivanen, M., & Lonnberg, H. (1990). Kinetics of reactions of pyrimidine nucleoside 2′- and 3′-monophosphates under acidic and neutral conditions: Concurrent phosphate migration, dephosphorylation and deamination. *Acta Chemica Scandinavica, 44*, 239–242. https://doi.org/10.3891/acta.chem.scand.44-023

Richter, Y., & Fischer, B. (2003). Characterization and elucidation of coordination requirements of adenine nucleotides complexes with Fe(II) ions. *Nucleosides, Nucleotides & Nucleic Acids, 22*, 1757–1780. https://doi.org/10.1081/NCN-120023271

Rohner, F., Ernst, F. O., Arnold, M., Hilbe, M., Biebinger, R., Ehrensperger, F., et al. (2007). Synthesis, characterization, and bioavailability in rats of ferric phosphate nanoparticles. *The Journal of Nutrition, 137*, 614–619. https://doi.org/10.1093/jn/137.3.614

Rossi, L., Velikov, K. P., & Philipse, A. P. (2014). Colloidal iron (III) pyrophosphate particles. *Food Chemistry, 151*, 243–247. https://doi.org/10.1016/j.foodchem.2013.11.050

Sabatini, A., Vacca, A., & Gans, P. (1974). Miniquad —a general computer programme for the computation of formation constants from potentiometric data. *Talanta, 21*, 53–77. https://doi.org/10.1016/0039-9140(74)80063-9

Sigel, H. (1990). Mechanistic aspects of the metal ion promoted hydrolysis of nucleoside 5'-triphosphates (NTPs). *Coordination Chemistry Reviews, 100*, 453–539. https://doi.org/10.1016/0010-8545(90)85018-N

Sigel, H., Massoud, S. S., & Corfu, N. A. (1994). Comparison of the extent of macrochelate formation in complexes of divalent metal ions with guanosine (GMP^{2-}), inosine (IMP^{2-}), and adenosine 5'-monophosphate (AMP^{2-}). The crucial role of N-7 basicity in metal ion-nucleic base recognition. *Journal of the American Chemical Society, 116*, 2958–2971. https://doi.org/10.1021/ja00086a028

Sun, Y., Zhao, L., & Teng, Y. (2020). Effect of soil type on the degradation of polychlorinated biphenyls in a pyrophosphate-chelated Fenton-like reaction. *Chemical Engineering Journal, 390*. https://doi.org/10.1016/j.cej.2020.124574. article 124574.

Sutyak, K. B., Zavalij, P. Y., Robinson, M. L., & Davis, J. T. (2016). Controlling molecularity and stability of hydrogen bonded G-quadruplexes by modulating the structure's periphery. *Chemical Communications, 52*, 11112–11115. https://doi.org/10.1039/C6CC06271G

Thakur, N., Sharma, B., Bishnoi, S., Jain, S., Nayak, D., & Sarma, T. K. (2019). Biocompatible Fe^{3+} and Ca^{2+} dual cross-linked G-quadruplex hydrogels as effective drug delivery system for pH-responsive sustained zero-order release of doxorubicin. *ACS Applied Bio Materials, 2*, 3300–3311. https://doi.org/10.1021/acsabm.9b00334

Thakur, N., Sharma, B., Bishnoi, S., Mishra, S. K., Nayak, D., Kumar, A., et al. (2018). Multifunctional inosine monophosphate coordinated metal–organic hydrogel: Multistimuli responsiveness, self-healing properties, and separation of water from organic solvents. *ACS Sustainable Chemistry & Engineering, 6*, 8659–8671. https://doi.org/10.1021/acssuschemeng.8b00963

Tian, T., Blanco, E., Smoukov, S. K., Velev, O. D., & Velikov, K. P. (2016). Dissolution behaviour of ferric pyrophosphate and its mixtures with soluble pyrophosphates: Potential strategy for increasing iron bioavailability. *Food Chemistry, 208*, 97–102. https://doi.org/10.1016/j.foodchem.2016.03.078

Xiao, S., & Davis, J. T. (2018). G_4-quartet hydrogels from 5′-hydrazino-guanosine for the non-covalent and covalent remediation of contaminants from water. *Faraday Discussions, 209*, 97–112. https://doi.org/10.1039/C8FD00038G

Zhang, F., Klebansky, B., Fine, R. M., Xu, H., Pronin, A., Liu, H., et al. (2008). Molecular mechanism for the umami taste synergism. *Proceedings of the National Academy of Sciences, 105*, 20930–20934. https://doi.org/10.1073/pnas.0810174106

Zhelyaskov, V., & Yue, K. T. (1992). A Raman study of the binding of Fe(III) to ATP and AMP. *Biochemical Journal, 287*, 561–566. https://doi.org/10.1042/bj2870561

Zhou, P., Shi, R., Yao, J.-F., Sheng, C.-F., & Li, H. (2015). Supramolecular self-assembly of nucleotide–metal coordination complexes: From simple molecules to nanomaterials. *Coordination Chemistry Reviews, 292*, 107–143. https://doi.org/10.1016/j.ccr.2015.02.007